Evaluation of Some Toxic Trace Elements in *Crocus Sativus* L. and Soil Using Neutron Activation Analysis Technique

Ehsan Taghizadeh Tousi

University of Torbat Heydarieh, Torbat Heydarieh, Iran Saffron Institute, University of Torbat Heydarieh, Torbat Heydarieh, Iran

Received: July 15, 2020/ Revised: November 2, 2022/ Accepted: November 24, 2022

Neutron activation analysis was used in this research to measure the concentrations of aluminum (Al), bromine (Br), chlorine (Cl), mercury (Hg), arsenic (As), and thorium (Th) in soil and saffron plants as well as their contamination, enrichment, and translocation rates. The edible part of the saffron showed a higher Hg concentration than the WHO/FAO-permitted level in the urban area. The soil was not intoxicated and contaminated by Al, As, and Th except in the urban areas, which were slightly polluted by As. The calculated contamination degree and pollution load index indicated that the soil was almost uncontaminated. The enrichment factors (EF) showed minimal enrichment levels of Al and Th and low As contamination, which may still increase due to human activities in the environment. The tested elements' translocation abilities were also evaluated by the paired t-test statistical method and indexes of translocation, and it was found that Al, As, and Th can quickly relocate into different soil depths. Saffron was also evaluated as a very poor absorber of the elements studied. While Cl and Th can easily move from the saffron's corm to its aerial parts, Al and Hg merely translocate from the corm to the petal. It was also found that Al, Cl, and Th can move between the petals and the thread.

Keywords: element translocation, enrichment, neutron activation analysis, soil contamination, trace elements

INTRODUCTION

Crocus sativus L., also known as saffron, is a perennial herbaceous plant of the monocot family Iridaceous family in the order Asparagales. Saffron grows through an onion named corm, which effloresces, with the flowers often blooming in purple in during the months of September and November. The red threads of saffron are the only edible and medicinal part of the plant and are typically consumed as a spice due to their significant nutritional benefits (Moratalla-López et al. 2019). The petal is also used as organic material in paint, cosmetics, pharmaceutics, and crafts (Hosseini et al. 2018). With its many uses in various industries, saffron is one of the most expensive agricultural products in the world. In Iran, it plays a unique role in non-oil exportation, and is annually cultivated in around 100,000 ha of Iranian farms. This yields about 340 tons of saffron, contributing to almost 90% of global saffron production (Koocheki and Seyyedi, 2015).

Although 20 out of 31 provinces in Iran have saffron farms, 90% of Iranian saffron is cultivated in the great Khorasan region, which includes three Khorasan provinces: North, Razavi, and South. The counties of Torbat-e Heydarieh and Zaveh located in Southwest Mashhad, the capital of Khorasan Razavi, were the first areas to produce saffron in Iran (Tousi 2022a); Torbat-e Heydarieh has an area of around 6,175 km² while Zaveh, initially a part of Torbat-e Heydarieh, has an area of around 2,437 km². Therefore, monitoring potentially harmful conditions which may lead to the elevation of trace element concentrations is important in controlling the quality of saffron exportation in Torbat-e Heydarieh and Zaveh and, consequently, Iran as a whole (Nepomuceno et al. 2020).

Trace elements are usually present in soils and plants, albeit in low concentrations. However, these concentrations may increase due to natural processes as well as human activities, consequently affecting soil and plant systems. One such trace element is aluminum (Al), which comprises nearly eight percent of the earth's crust.

^{*}Author for correspondence; Email: e.taghizadeh@torbath.ac.ir; ORCID: https://orcid.org/ 0000-0001-9608-9406

Aluminum can enter the life cycle of plants since it is also used as a precipitating substance in water treatment. It has a very complex function in biological processes and is absorbed by the plants roots through increasing soil and atmosphere contamination as well as acid rain absorption (Kabata-Pendias 2011). The toxicity of aluminum has also been found to affect different cellular structures across plant species, and studies have shown that it increases the risk of developing pulmonary and kidney disease as well as Alzheimer's in humans (Tohidi et al. 2015; Singh et al. 2017).

Bromine is another vital element for living organisms (Mohd-Taufek et al. 2016). However, excessive bromine concentration can be toxic to humans, posing significant risks for the nervous system and the thyroid gland (Slotkin et al. 2017). The maximum level of bromine in food was determined by the World Health Organization (WHO) to be 50 mg/kg (WHO 2018), and soil with a bromine concentration higher than this recommended level is considered contaminated for plant growth (Shtangeeva et al. 2017).

Chlorine, an element present in the earth's crust with an average value of approximately 470 mg/kg (Shimizu et al. 2016), also occurs in plants as chloride (Cl-) (FAO 2006). Although irrigation water is the primary cause of plant contamination by chlorine (Allende and Monaghan 2015), plants can also be contaminated by chlorine in the air (Wyczarska-Kokot et al. 2017). While 100 mg/kg of chloride is seriously essential for plants' chemical processes (Esna-Ashari and Gholami 2010), concentrations above the WHO-recommended level of 500 - 1,000 mg/kg (WHO 2003) are considered toxic and can cause necrosis of plant tissue (White and Broadley 2001). Osmoregulation, photosynthesis, and cell division are also affected by plant chlorine concentration (Franco-Navarro et al. 2015).

Mercury (Hg) is one of the most severely toxic heavy metals and has various detrimental effects on humans, ranging from nausea and loss of balance to irreversible brain damage (Bernhoft 2012). The maximum Hg concentrations have been defined as 20 μ g/kg and 20 μ g/kg for human and animal feed, respectively (WHO 2000; MHPRC 2012).

Human activities have also further increased the risk of contamination by arsenic, another heavy metal that is naturally present as a contaminant mineral (Tousi, Hashim et al. 2014). Arsenic exposure is a significant global health concern (Rasheed et al. 2016), and careful monitoring of arsenic levels must be implemented to ensure that they do not exceed 0.01 mg/Ll in drinking

water (WHO 2011), 1 mg/kg in food (Barua et al. 2010), and 40 mg/kg in soil (Yaffee et al. 2019).

Thorium is one of nature's most abundant radioactive elements (Tousi et al. 2016), with a mean range of 8 – 12 mg/kg present in the earth's crust (Omoniyi et al. 2013). Several researchers have also investigated thorium concentrations in various foods for human and animal consumption, and it was found that values of less than 5 mg/kg were present in uncontaminated foods (Misdaq and Bourzik 2004; Oufni et al. 2011; Zehringer 2020).

The amount of such trace elements in soil samples can be determined through neutron activation analysis (NAA), a sensitive analytical technique which makes use of radioactive decay to identify which elements are present in a sample and precisely calculate their respective quantities. Radioactive decay is achieved through the activation or creation of isotopes generated when a non-charged neutron bombards the target nucleus in the sample material (Minc 2008). This neutron source consists of radioisotope, the neutron generator, and the nuclear reactor (Tousi, Kardani et al. 2014). NAA is considered a highly reliable technique due to its precision and accuracy, as errors of only 2 – 5% relative standard deviation can be achieved for various elements (USGS 2023).

This study was conducted to determine and evaluate the concentrations of the above-mentioned toxic elements in saffron and soil samples using NAA. Likewise, these elements' contamination, enrichment, and translocation values were measured using appropriate statistical analyses and environmental indexes.

MATERIALS AND METHODS

Sample Collection and Preparation

Saffron plant samples used for the study consisted of (a) the corm, (b) red threads, and (c) herbaceous specimens (including petals, leaves, and stems). The saffron corms were cultivated at a depth of 15 – 20 cm (Colla and Rouphael 2009) using a garden shovel and scissors while soil samples, which included (a) topsoil of up to 15 cm in depth and (b) soil at a depth of 15 – 30 cm, were collected from the study area using a manual earth auger (Fig. 1). Specific sites were determined through stratified random sampling (Cao et al. 2016; Marín et al., 2017; Zhao et al. 2019; Boente et al. 2020; Tousi, 2020) based on the north, center, and south zones of Torbat Heydarieh and the west, center, and east zones of Zaveh in Iran. The areas of the two counties were approximately 2,000 and 700 ha, respectively, and were divided into nine sections.



Fig. 1. Schematic diagram of the classification of studied areas.

The saffron farms with the top cultivation and production rates were then identified based on the highest amount of harvests per hectare three years before the research was conducted. At least five different sampling points per farm were further selected.

Based on the top cultivation, 50 – 100 farms were selected in each part. Accordingly, 200 farms were chosen in each county, which were sampled at five various spots. A composite sample was then prepared for each farm by mixing five types. Following the method of Barragán et al. (2018), 25 parts were homogenously blended to further create mixture samples, amounting to a total of 120 samples for the five types. These were washed with distilled water, and the moisture was decreased by air-drying for 2 wks. The plant samples were then crushed using an electric grinder and were made into powder using a ceramic mortar and pestle. A sieve shaker was finally used to sort the samples. Then, each sample was packed and labeled for injection into the TRR core.

Neutron Activation Analysis (NAA)

In this study, channels A, D, E, and G were used, each with cylinders with having 6 in radii. The commonly used NAA method is the relative NAA to avoid intricate calculations, which compares the sample activity with a standard. Eq. 1 is the main formula of the relative NAA (Tousi et al., 2016).

$$\begin{aligned} & \text{Sample:} A_{sam} = \varphi \sigma N_{sam} (1 - e^{-\lambda t_i}) (e^{-\lambda t_d}) \\ & \text{Standard:} A_{st} = \varphi \sigma N_{st} (1 - e^{-\lambda t_i}) (e^{-\lambda t_d}) \end{aligned} \\ & \Rightarrow \frac{A_{sam}}{A_{st}} = \frac{N_{sam}}{N_{st}} = \frac{W_{sam}}{W_{st}} \Rightarrow D = \frac{W_{sam}}{G} = \frac{W_{st}}{G} \frac{A_{sam}}{A_{st}} \end{aligned} \tag{1}$$

where A (activity of nuclei); W (weight of nuclei); N (number of nuclei); σ (neutron cross-section); θ (isotopic abundance); λ (decay constant); G (total mass); and D (weight concentration). The times of irradiation and decay are respectively shown by t_i and t_d . The precision of the NAA's results was estimated by the relative standard deviation (RSD) , which is measured by Eq. 2 (Dong et al. 2017)

RSD =
$$[\delta/(Mean \text{ of Data})] \times 100$$
 (2)

where the standard deviation of the repeated results is shown by δ . The NAA-measured concentrations of

elements in the reference samples (multi-element standard) were compared with their confirmed values to evaluate the NAA results' accuracy (Syahfitri et al. 2017).

Statistical Methods

Previous studies have recommended the paired t-test for the evaluation of the similarity of spectroscopy results such as X-ray fluorescence (XRF) and NAA methods (Abuarra, Bauk, Hashim, Kandaiya, Tousi, Ababneh 2014; Al-Jarrah et al. 2016; Zaichick and Zaichick 2016; Mádlíková et al. 2018; Tousi, 2022b). In this study, the paired t-test was selected for its suitability for a statistical population with less than 30 samples (Sayfi and Nikbakht 2016; Tousi et al. 2018). The t-test can be applied to one sample under some treatments (Blaeschke et al. 2018; Tousi et al. 2015). Hence, it was used in this study to determine the transfer rate of trace elements among the five different sample types: (1) surface soil (depth up to 15 cm), (2) surrounding soil of corm (depth of 15 – 30 cm), (3) corm, (4) petal, and (5) the red saffron.

The concentrations of trace elements in each sample type were compared. The null hypothesis (H_0) states that the average difference between the values of this trace element in two kinds of samples is zero. If the p-values were more than 0.05, H_0 would be accepted (Tousi et al. 2017). An accepted null hypothesis indicates that the element concentrations in the two sample types were statistically equivalent, which would explain the excellent transition of this element between the two sample types (Tousi, Bauk et al. 2014).

Soil Contamination Level

In this research, the contamination factor (CF) was applied as a simple and effective pollution index in soil samples and was calculated using Eq. 3 (Jose and Srimuruganandam 2020), where C_i is the average concentration of an ith element in the soil samples of an area and GB_i is that of the world average shale values (ASV) (Remeikaitė-Nikienė et al. 2018). Previous works have classified the main parent material of the soils in the Torbat Heydarieh and Zaveh counties as sedimentary rocks which are mostly shale (Nouraliee 2005; Malekzadeh Shafaroudi et al. 2022).

$$CF_i = C_i/GB_i$$
 (3)

The CF indicates the soil contamination condition by a single element. The contamination level of soil has been classified as follows: CF < 1—uncontaminated, $1 \le CF < 3$ — moderate pollution, $3 \le CF < 6$ — high contamination, and $6 \le CF$ — extremely contaminated (Kowalska et al. 2018). The summation of the contamination factors of all

studied elements has been recommended to evaluate the total soil contamination level in an area, which is called the contamination degree (CD) (Kowalska et al. 2018). CD < 8, $8 \le$ CD < 16, $16 \le$ CD < 32, and $32 \le$ CD indicate uncontaminated, moderate, high, and extreme total contamination levels of soil, respectively (Kowalska et al. 2018).

Contamination factors and degrees are the applied indexes as these are simple, suitable, and applicable to estimating the environmental condition of an area. The second group of contamination indexes is recommended to improve the accuracy and levels of the determination of the contamination class. Therefore, the geo-accumulation index (I-geo) was defined by Eq. 4, where the coefficient 1.5 is a correction factor for lithological variations (Masto et al. 2019).

$$Igeo_i = \log_2[C_i/(1.5 \times GB_i)] \qquad (4)$$

The total contamination of soil can also be determined by the pollution load index (PLI), which is the geometric average of the contamination index. Eq. 5 calculates PLI, where n is the number of analyzed elements (Masto et al. 2019). The soil situation can be easily assessed by PLI (Rai et al. 2019). The geoaccumulation index (such as the contamination factor) shows the level of soil contamination by a single element. However, the pollution load index and contamination degree display the soil's total contamination by all the studied elements. Table 1 shows the classification of soil contamination levels based on the I-geo and PLI values (Malinowska et al. 2015; Rai et al. 2019).

$$PLI = \sqrt[n]{CF_1 \times CF_2 \times \cdots CF_n}$$
 (5)

Soil Enrichment Factor

The enrichment factor (EF) has been recommended for the evaluation of the sedimentation of an element in the soil. The EF is calculated by Eq. 6, where C_i , GB_i , and CF_i are related to the element in Eq. 4 (Remeikaitė-Nikienė et al. 2018). Also, ref indicates the reference element (Zinkutė et al. 2017).

Table 1. Contamination level of the soil.

Class	Contamination Rate	l-geo ^a	PLIb
0	Uncontaminated	I-geo≤0	0≤PLI<1
1	None/Moderately pollution	0 <i-geo≤1< td=""><td>1≤PLI<2</td></i-geo≤1<>	1≤PLI<2
2	Moderately pollution	1 <i-geo≤2< td=""><td>2≤PLI<3</td></i-geo≤2<>	2≤PLI<3
3	Moderately/Strongly pollution	2 <i-geo≤3< td=""><td>3≤PLI<4</td></i-geo≤3<>	3≤PLI<4
4	Strongly pollution	3 <i-geo≤4< td=""><td>4≤PLI<5</td></i-geo≤4<>	4≤PLI<5
5	Strongly/Extremely pollution	4 <l-geo≤5< td=""><td>5≤PLI<6</td></l-geo≤5<>	5≤PLI<6
6	Extremely pollution	5 <i-geo< td=""><td>6≤PLI</td></i-geo<>	6≤PLI

 $^{^{\}rm a}$ (Malinowska et al., 2015); $^{\rm b}$ (Rai et al., 2019); Geo-accumulation index (I-geo); Pollution load index (PLI)

$$EF_i = (C/C_{ref})/(GB/GB_{ref}) = (C/GB_i)/(C_{ref}GB_{ref}) = CF_i/CF_{ref}$$
 (6)

The reference element is an immobile element such as aluminum (Al), iron (Fe), and silicon (Si) (Ita and Anwana 2017). Many researchers have widely chosen to measure the enrichment factor of another element (Mondal et al. 2020). The value $0.5 < EF \le 1.5$ merely refers to the effects of natural activities without anthropogenic influence on the changing elemental distribution in the environment (Kłos et al. 2011). Hence, EF < 0.5, $0.5 \le EF < 2$, $2 \le EF < 5$, $5 \le EF < 20$, $20 \le EF < 40$, and $40 \le EF$ indicate the deficiency, minimal, moderate, significant, very high, and extremely high enrichment levels, respectively (Barbieri 2016).

Evaluation of Elements' Translocation Ability

The translocation indexes of a mineral can be classified into two main groups: (a) from the soil to the plant and (b) between the various parts of the plant. The biological accumulation factor (BAF) evaluates an element's translocation ability from the soil to the parts of the plant, which is measured by Eq. 7 (Kumar et al. 2020). The BAF identifies the translocation indexes from all exposure paths such as soil, water, and air (Borgå 2013). The values 1 < BAF or BAF < 1 imply that the plant would be a good or poor accumulator of an element, respectively (Kazi et al. 2019).

$$BAF = (Element in plant parts)/(Element in soil)$$
 (7)

An element's translocation ability of a plant from the root to the aerial parts is estimated by the translocation factor (TF) value, which is calculated by Eq. 8. A plant is categorized as a metal hyperaccumulator from the roots to the aerial parts of a plant if the translocation factor is greater than one (Coakley et al. 2019).

$$TF = (Element in aerial parts)/(Element in root)$$
 (8)

RESULTS AND DISCUSSION

The accuracy and precision of the NAA results were estimated by 10 repeated measurements of three known multi-element samples as the TRR reactor's standard samples. Afterward, the relative standard deviations (RSD) and average relative standard deviation (ARSD) of each element for the six minerals were computed using Eq. 2, and the precision of the method's results increased as the RSD decreased. Although the precision of the analytics' results is usually accepted by ARSD \leq 20% (McKenna et al. 2020), the International Atomic Energy Agency (IAEA) has recommended ARSD \leq 10% for the results of NAA in biomedical and biophysics (Parr 1984). The average relative standard deviation values (ARSD) for all elements were \leq 5% which indicates the high

precision of NAA in determining the concentration of Al, Br, Cl, Hg, As, and Th in the saffron and soil samples. The accuracy of NAA was proved by the low standard deviation and the relative error of elements' concentrations between measured and confirmed concentrations of elements in the reference samples (multi-element standard). Past studies have also demonstrated NAA's high accuracy and precision in specifying the trace elements in biological samples (Dybczyński 2019).

The mean values of aluminum, bromine, chlorine, mercury, arsenic, and thorium concentrations for two types of soil samples and three types of saffron samples in the six zones of Torbat Heydarieh and Zaveh was shown in Fig. 2. The permitted aluminum level of the soil is strongly affected by the soil's pH-aluminum toxicity appears in acidic soils with pH levels of <5.5, at which the toxicity level of Al in the soil is more than 3 mg/kg (Rout et al. 2001). The concentrations of Al in the soil samples are illustrated in Fig. 2a, which shows that the measured contents in all soil samples were significantly higher than the aforementioned standard. Then, the pH values of the soil solution using a 1:5 soil-water ratio were determined by a pH meter model of 86502Az and were found to be higher than 6.5. Hence, the high aluminum concentrations were non-toxic for plants in all the saffron farms of Torbat Heydariyeh and Zaveh.

The provisional tolerable weekly intake (PTWI) of aluminum is 0.9 mg/L in drinking water. Also, aluminum's PTWI is 50 mg for each kg of body weight in feed, which means the Al content of food cannot exceed 1,000 mg/kg for children and 4000 mg/kg for adults as the maximum permissible level (MPL) (Stahl et al. 2011). The aluminum levels of various parts of saffron are shown in Fig. 2b. However, the aluminum levels of the corm and petal of saffron as the non-edible parts exceeded 1,000 mg/kg, which indicates the non-toxicity of aluminum in all parts of the saffron plant in Torbat Heydarieh and Zaveh.

Bromine, chlorine, and mercury were not found in the soil samples based on the neutron activation analysis. Fig. 2c depicts the concentrations of Br in the threads, petals, and corms of saffron. The maximum permissible level of bromine in the edible parts of the plant is around 50 mg/kg (WHO et al. 2018). Therefore, the saffron plants were uncontaminated by bromine in all study areas.

Chlorine concentrations in various parts of the saffron plant are shown in Fig. 2d. The threads' chlorine values were approximately 700 - 850 mg/kg, which were in the allowable range for edibility (100 - 1,000 mg/kg) (WHO

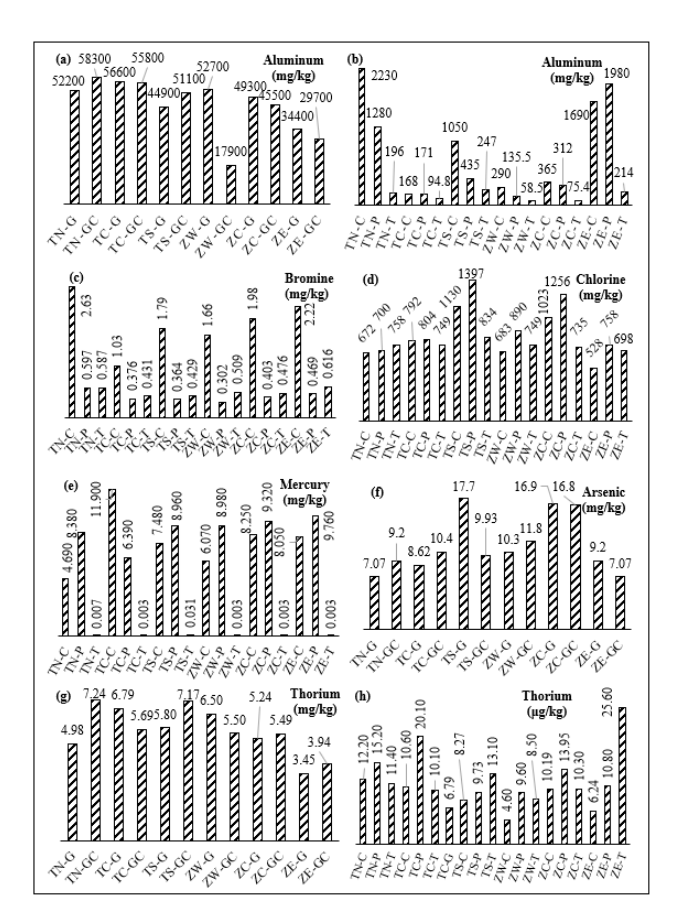


Fig. 2. (a) Aluminium in the soil; (b) Al in saffron; (c) Bromine in saffron; (d) Chlorine in saffron; (e) Mercury in saffron; (f) Arsenic in the soil; (g) Thorium in the soil; and (h) Thorium in saffron; TN: North of Thorbat Heydarieh; TC: Center of Thorbat Heydarieh; TS: South of Thorbat Heydarieh; ZW: West of Zaveh; ZC: Center of Zaveh; ZE: East of Zaveh; G: Topsoil; GC: Soil around the corm; C: Saffron corm; P: Saffron petal; and T: Saffron threads.

2003; Esna-Ashari and Gholami 2010). The chlorine concentrations in the petal and corm were higher than the MPL in the south of Torbat Heydarieh and the center of Zaveh, which are urban areas. Natural chlorine sources commonly include rainwater, irrigation waters, dust, and the atmosphere. Although Cl was not found in the soil samples in all study zones, the Cl concentrations of the various plant parts were almost high (528 – 1,397 mg/kg). Human activities such as irrigation with polluted water, air pollution, and chloride-containing fertilizers can significantly contaminate plants with Cl. However, in this research, the high level of chlorine in some study areas may have been caused by a combination of all the factors mentioned above, and it is not possible to accurately determine the contribution of each of them.

The concentration of mercury in the various parts of saffron is shown in Fig. 2e. The MPL of Hg is 20 μ g/kg in human feed and 20 mg/kg in animal feed (WHO 2000;

MHPRC 2012). Accordingly, the Hg level of threads south of Torbat Heydarieh county exceeded the MPL. The mercury in the non-edible organs of saffron (petal and corm) was less than 20 mg/kg, which means that the corm and petal of saffron were not contaminated by mercury. In all the study zones, the Hg concentrations in the corm and petals were much higher than those in the threads which shows that mercury can be translocated to and can accumulate in the non-edible parts of saffron (Fig. 2e). Initially, the primary source of mercury in nature was volcanism; nowadays, Hg is sourced through the retranslocation from formerly deposited mercury on the surface of the earth's crust (Clemens 2013). Currently, one of the main sources of mercury is greenhouse gases, which are caused by natural fires and fossil-based fuels (Pirrone et al. 2010). Former studies have indicated that mercury can be absorbed by plants through the air and the soil (Li et al. 2017). In this study, Hg was not found in the soil samples. Therefore, air pollution can be the main factor in the absorption of mercury by saffron, which is supported by previous studies (Pirrone et al. 2010; Li et al. 2017). Moreover, Iran has huge resources for fossil fuels; hence, it is possible that the high use of cheap fossil fuels is another significant contributor to the high mercury content in saffron.

The NAA revealed the absence of arsenic in the saffron plant samples, thus making saffron a poor arsenic accumulator. The concentration levels of arsenic in the soil samples taken from the saffron farms levels at 0-15 cm and 15-30 cm depths were less than the recommended value of 40 mg/kg (Yaffee et al. 2019), implying the non-toxicity of arsenic in Torbat Heydareih and Zaveh (Fig. 2f).

The soil samples from all saffron farms of Torbat Heydarieh and Zaveh contained 3.45–7.24 mg/kg of thorium, indicating non-toxicity (Fig. 2g). Moreover, the concentrations of thorium in various parts of the saffron plant ranged between $4.60-25.60~\mu g/kg$, which were less than the recommended value of 5 mg/kg for edibility (Fig. 2h). Conclusively, the saffron plants and the soils from saffron farms were not contaminated by aluminum, bromine, chlorine, mercury, arsenic, and thorium in all areas of Torbat Heydarieh and Zaveh.

Soil Contamination and Enrichment

Four indicators were used to determine the soil pollution conditions of the saffron farms. Aluminum, arsenic, and thorium were found in the farmland. The global average shale values (ASV) of aluminum, arsenic, and thorium are 80,000 mg/kg (Salomons and Förstner 1984), 8.6 mg/kg (Armstrong et al. 2019), and 12 mg/kg (Aziz et al. 2019),

Table 2. Two factors to evaluate the contamination of soil by a single metal: Contamination Factor (CF) and Index of Geo-accumulation (I-geo).

Factors Element			Study areas						
		TN	TC	TS	ZW	ZC	ZE	Mean	
	Al	0.07	0.07	0.06	0.04	0.06	0.04	0.06	
CF	As	0.95	1.11	1.61	1.28	1.96	0.95	1.31	
	Th	0.51	0.52	0.54	0.5	0.45	0.31	0.47	
	Al	-0.27	-0.27	-0.29	-0.31	-0.29	-0.32	-0.29	
l-geo	As	-0.21	-0.14	0.03	-0.07	0.12	-0.21	-0.08	
	Th	-1.56	-1.53	-1.47	-1.58	-1.74	-2.27	-1.69	

TN: North of Thorbat Heydarieh; TC: Center of Thorbat Heydarieh; TS: South of Thorbat Heydarieh; ZW: West of Zaveh; ZC: Center of Zaveh; ZE: East of Zaveh.

respectively. Table 2 shows the measured contamination factor (CF) values of arsenic, aluminum, and thorium in the six sites studied, which were calculated using Eq. 3.

The means of the soils' CF for aluminum, arsenic, and thorium were 0.68, 1.31, and 0.47, respectively. Likewise, all of the calculated soils' CF values for aluminum and thorium were approximately CF < 1, which indicates no contamination in the counties of Torbat Heydarieh and Zaveh. The arsenic CF of soil (except in Northern Torbab Heydarieh and Eastern Zaveh) was calculated between 1 and 2 with the mean being 1.31, indicating moderate arsenic pollution at $1 \le CF < 3$.

The soil's geo-accumulation index (I-geo) was calculated using Eq. 4 to assess the metals' ecological risks (Table 2). The soil I-geo of all farms was found to be negative for aluminum, arsenic, and thorium, except for the I-geo of soil for arsenic in the urban areas of the two counties. Hence, both indexes of I-geo and CF display non-pollution of soil by aluminum and thorium.

The measured soil contamination degrees (CD) of saffron farms ranged from 1.30 - 2.47, with an average of 1.84, indicating non-contamination (Table 3). The pollution load index (PLI) was also applied for the total assessment of the level of soil contamination. The PLI values of all studied areas were measured as < 1.

Pollution indicators including CF, I-geo, CD, and PLI express the current soil pollution conditions. Aside from these, the enrichment factor (EF) has also been a recommended metric to detect the process of increasing

Table 3. Two factors to evaluate the total contamination of soil: Contamination Degree (CD) and Pollution Load Index (PLI).

Easters -	Study Areas							
Factors	TN	TC	TS	ZW	ZC	ZE	Mean	
CD	1.52	1.7	2.21	1.82	2.47	1.3	1.84	
PLI	0.32	0.34	0.37	0.3	0.37	0.23	0.32	

TN: North of Thorbat Heydarieh; TC: Center of Thorbat Heydarieh; TS: South of Thorbat Heydarieh; ZW: West of Zaveh; ZC: Center of Zaveh; ZE: East of Zaveh.

or decreasing soil contamination of an area by an element, which refers to the sedimentation rate of the element in an area. In this research, iron was selected as an immobile reference element to estimate the EF values of aluminum, arsenic, and thorium. Using Eq. 3., the CF of the soils for iron were measured along with the mean concentrations in the soils of each studied zone (Table 4). These values were also compared to the global average shale value (ASV) of iron, which has been recorded at 47,200 mg/kg (Salomons and Förstner 1984).

The EF values of aluminum and thorium were < 1.5 in all the study areas, indicating minimal enrichment (Table 5). This result implies that human activities have not directly affected the changes in the concentrations of aluminum and thorium in Torbat Heydarieh and Zaveh. The EF values of arsenic in Southern Torbat Heydarieh and in Western and Central Zaveh (> 1.5) also show that the element's presence in the soil is a mere effect of natural conditions. However, these sites are urban areas connected to Western Zaveh where there are existing porcelain industries, sugar beet factories, oil refineries, industrial estates, and cement companies, which may eventually lead to moderate arsenic sedimentation.

Displacement Estimation

From the six studied elements, only aluminum, arsenic, and thorium were found to be present in the soils of the saffron farms. Table 6 shows the *p*-values of the statistical pairs for an element in different soil depths. Accordingly, the concentrations of aluminum, arsenic, and thorium

Table 4. Concentration and contamination factors (CF) of the soils' iron.

	TN	TC	TS	ZW	ZC	ZE
Fe (mg/kg)	39450	40700	33450	28800	35050	37050
CF _{Fe}	0.84	0.86	0.71	0.61	0.74	0.79

World average shale value of iron: 47200 mg/kg (Salomons and Förstner, 2012); TN: North of Thorbat Heydarieh; TC: Center of Thorbat Heydarieh; TS: South of Thorbat Heydarieh; ZW: West of Zaveh; ZC: Center of Zaveh; ZE: East of Zaveh.

Table 5. Enrichment factors (EF) to estimate the sedimentation intensity of metal in the soil of the saffron farm.

Eastara	Element -	Study Areas						
raciois	Element -	TN	TC	TS	ZW	ZC	ZE	Mean
	Al	0.08	0.08	0.08	0.07	0.08	0.05	0.08
EF	As	1.13	1.28	2.27	2.11	2.64	1.21	1.77
	Th	0.61	0.6	0.76	0.82	0.61	0.39	0.63

TN: North of Thorbat Heydarieh; TC: Center of Thorbat Heydarieh; TS: South of Thorbat Heydarieh; ZW: West of Zaveh; ZC: Center of Zaveh; ZE: East of Zaveh.

Table 6. P-values of the pair of soils for aluminum (Al), arsenic (As), and thorium (Th).

Name of Pair	Al	As	Th
Topsoil-Soil of Corm	0.432	0.423	0.512

were statistically equivalent across various soil depths, which imply the elements' good displacement abilities into the soils. These uniform distributions may be explained by the geological nature of the two counties.

Results from the NAA also showed that aluminum and thorium were detected in both soil and plant samples (Table 7). The *p*-values were between 0.000 to 0.011, indicating that the concentration of both metals in the soil and saffron samples was not statistically equivalent.

The bioaccumulation factors for corm (BAF-C), petal (BAF-P), and threads (BAF-T) were also explored in this study (Table 8). The average values of BCA-C were calculated to be 0.022 and 0.002 for aluminum and thorium, respectively. Also, the means of measured BAF-P and BAF-T values for both metals were 0.002-0.018, indicating that saffron is a poor accumulator of aluminum and thorium. The measured BAFs in Table 8 further affirm the t-test results in Table 7.

Aluminum, bromine, chlorine, mercury, and thorium were also found in various parts of the saffron plant. Table 9 shows the p-values of the statistical pairs for the different parts of the saffron plant, while Table 10 shows the translocation factor (TF) values for the petal and thread of the saffron plant. The average TF-P values for Cl, Hg, and Th were > 1, indicating good translocation abilities from corm to petal. Also, the t-test results revealed that the concentrations of Cl, Hg, and Th were statistically similar in the corm and petal, showing the uniformity of accumulation in these parts of the saffron plant.

Table 7. P-values of the plant pairs for aluminum (Al) and thorium (Th).

tiioriaiii (i ii).		
Name of Pair	Al	Th
Corm-Topsoil	0	0.011
Petal-Topsoil	0	0.001
Threads-Topsoil	0	0.001
Corm-Soil of Corm	0.001	0.001
Petal-Soil of Corm	0.001	0.001
Threads-Soil of Corm	0.001	0.001

Table 8. Bioaccumulation factors for corm (BAF-C), petal (BAF-P), and threads (BAF-T) of the saffron plant.

Factors	Flament		Study Areas						
	Licinciit	TN	TC	TS	ZW	ZC	ZE	Mean	
BAF-C	Al	0.04	0.003	0.022	0.008	0.008	0.053	0.022	
	Th	0.002	0.002	0.002	0.002	0.002	0.003	0.002	
BAF-P	Al	0.023	0.003	0.009	0.004	0.007	0.062	0.018	
	Th	0.002	0.003	0.002	0.002	0.003	0.003	0.003	
BAF-T	Al	0.004	0.002	0.005	0.002	0.002	0.007	0.003	
	Th	0.002	0.002	0.002	0.001	0.002	0.004	0.002	

TN: North of Thorbat Heydarieh; TC: Center of Thorbat Heydarieh; TS: South of Thorbat Heydarieh; ZW: West of Zaveh; ZC: Center of Zaveh; ZE: East of Zaveh.

Table 9. T-test results of the plant.

Name of Pair	Al	Br	CI	Hg	Th
Corm-Petal	0.24	0.001	0.106	0.535	0.05
Corm- Threads	0.049	0.001	0.559	0.001	0.052
Petal-Threads	0.101	0.035	0.103	0	0.512

Table 10. Translocation factor (TF) for the petal (TF-P), and threads (TF-T) of the saffron plant.

Factors Element -			Study Areas							
		TN	TC	TS	ZW	ZC	ZE	Mean		
	Al	0.57	1.02	0.41	0.47	0.85	1.17	0.75		
	Br	0.23	0.37	0.20	0.18	0.20	0.21	0.23		
TF-P	CI	1.04	1.02	1.24	1.3	1.23	1.44	1.21		
	Hg	1.79	0.54	1.20	1.48	1.13	1.21	1.22		
	Th	1.25	1.90	1.18	2.09	1.36	1.73	1.62		
	Al	0.09	0.56	0.24	0.2	0.21	0.13	0.24		
	Br	0.22	0.42	0.24	0.31	0.24	0.28	0.28		
TF-T	CI	1.13	0.66	0.74	0.73	0.72	1.32	0.88		
	Hg	0.00	0.00	0.00	0.00	0.00	0.00	0.00		
	Th	0.93	0.95	1.58	1.85	1.90	4.10	1.89		

TN: North of Thorbat Heydarieh; TC: Center of Thorbat Heydarieh; TS: South of Thorbat Heydarieh; ZW: West of Zaveh; ZC: Center of Zaveh; ZE: East of Zaveh.

The p-values of the corm-threads pair were > 0.05 for chlorine and thorium, indicating comparable concentrations of these elements. Similarly, the TF values illustrate good thorium accumulation and movement into the saffron threads, confirming the t-test results in Table 9 (Table 10). Finally, Al, Cl, and Th were found to be able to move quickly from the petals to the threads of saffron.

CONCLUSION

In this research, neutron activation analysis (NAA) was used to measure the concentrations of aluminum (Al), bromine (Br), chlorine (Cl), mercury (Hg), arsenic (As), and thorium (Th) in various parts of the saffron plant and also at different soil depths. Al, Br, Cl, and Th concentrations in the red threads were lower than the FAO/WHO maximum permissible level (MPL). Further, the Hg levels in the red threads were lower than the MPL except in the urban part of Torbat Heydarieh, which could be caused by city pollution and oil refineries. Arsenic was not found in the saffron plant, while Br, Cl, and Hg were not detected in the soil samples. There was no contamination with Al, As, and Th in the soil, which was supported by the calculated contamination factor (CF) and geo-accumulation index (I -geo) values generated by the study. The urban areas also exhibited minimal pollution by As as supported by the contamination degree (CD) and pollution load index (PLI) values. Likewise, the enrichment factor (EF) values indicated minimal enrichment of the soil by the studied elements except for As, with an EF of > 1.5 in the urban and industrial areas of Southern Torbat Heydarieh and Western and Central Zaveh and which may still increase because of human activities. The translocation factor (TF) and bioaccumulation factor (BAF) values also revealed that Cl, Hg, and Th can lightly move from the corm to the petal, and that Cl and Th can move well from the corm to the threads and between the aerial parts of saffron.

ACKNOWLEDGMENT

The University of Torbat Heydarieh has financially supported this research. The grant number was UTH:1399/03/02474.

REFERENCES CITED

ABUARRA A, BAUK S, HASHIM R, KANDAIYA S, TOUSI ET, ABABNEH B. 2014. XRF technique for the evaluation of gum arabic bonded *Rhizophora* spp. particleboards as tissue equivalent material. Int J Appl Phys Math. 4(3):201-204. doi:10.7763/IJAPM.2014.V4.283.

ABUARRA A, BAUK S, HASHIM R, KANDAIYA S, TOUSI ET, ALDROOBI K. 2014. Microstructure examination, elemental composition analysis of gum arabic bonded *Rhizophora* spp. particleboards and their potential as tissue equivalent material. Int J Chem Environ Biol Sci. 2(1):71-75. https://www.researchgate.net/publication/263659580_Microstructure_Examination_

Elemental_Composition_Analysis_of_Gum_Arabic_B onded_Rhizophora_Spp_Particleboards_and_Their_P otential_as_Tissue_Equivalent_Material.

AL-JARRAH AM, RAHMAN AA, SHAHRIM I, AB RAZAK NNAN, ABABNEH B, TOUSI ET. 2016. Effect of inorganic salts and glucose additives on dose –response, melting point and mass density of genipin gel dosimeters. Phys Medica. 32(1):36-41. doi:10.1016/j.ejmp.2015.09.003.

ALLENDE A, MONAGHAN J. 2015. Irrigation water quality for leafy crops: a perspective of risks and potential solutions. Int J Environ Res Pub He. 12 (7):7457-7477. doi:10.3390/ijerph120707457.

ARMSTRONG JGT, PARNELL J, BULLOCK LA, BOYCE AJ, PEREZ M, FELDMANN J. 2019. Mobilization of arsenic, selenium, and uranium from carboniferous black shales in west Ireland. Applied Geochemistry. 109:104401. doi:10.1016/j.apgeochem.2019.104401.

AZIZ A, ATTIA T, MCNAMARA L, FRIEDMAN R. 2019. Application of gamma-ray spectrometry in discovering the granitic monument of King Pepi I: a

- case study from Hierakonpolis, Aswan, Egypt. Pure Appl Geophys. 176:1639-1647. doi: 10.1007/s00024-018-2036-1.
- BARBIERI M. 2016. The importance of enrichment fact (EF) and geoaccumulation index (Igeo) to evaluate the soil contamination. J Geol Geophys. 5:1-4. doi:10.4172/2381-8719.1000237.
- BARRAGÁN C, WETZEL CE, ECTOR L. 2018. A standard method for the routine sampling of terrestrial diatom communities for soil quality assessment. J Appl Phycol. 30:1095-1113. doi:10.1007/s10811-017-1336-7.
- BARUA A, GUPTA SD, MRIDHA MAU, BHUIYAN MK. 2010. Effect of arbuscular mycorrhizal fungi on growth of *Gmelina arborea* in arsenic-contaminated soil. J Forestry Res. 21:423-432. doi:10.1007/s11676-010 -0092-1.
- BERNHOFT RA. 2012. Mercury toxicity and treatment: a review of the literature. J Environ Pub He. 2012:460508. doi:10.1155/2012/460508.
- BLAESCHKE F, STENGER D, KAEUFERLE T, WILLIER S, LOTFI R, KAISER AD, ASSENMACHER M, DÖRING M, FEUCHT J, FEUCHTINGER T. 2018. Induction of a central memory and stem cell memory phenotype in functionally active CD4+ and CD8+ CAR T cells produced in an automated good manufacturing practice system for the treatment of CD19+ acute lymphoblastic leukemia. Cancer Immunology, Immunotherapy. 67(7):1053-1066. doi:10.1007/s00262-018-2155-7.
- BOENTE C, MARTÍN-MÉNDEZ I, BEL-LAN A, GALLEGO JR. 2020. A novel and synergistic geostatistical approach to identify sources and cores of potentially toxic elements in soils: an application in the region of Cantabria (Northern Spain). J Geochem Explor. 208:106397. doi:10.1016/j.gexplo.2019.106397.
- BORGÅ K. 2013. Ecotoxicology: bioaccumulation. In: Elias S, editor. Reference module in Earth systems and environmental sciences. Elsevier. p. 346-348.
- CAO J, GAO Z, YAN J, LI M, SU J, XU J, YAN CH. 2016. Evaluation of trace elements and their relationship with growth and development of young children. Biol Trace Elem Res. 171(2):270-274. doi:10.1007/s12011-015-0537-7.
- COAKLEY S, CAHILL G, ENRIGHT AM, O'ROURKE B, PETTI C. 2019. Cadmium hyperaccumulation and

- translocation in *Impatiens glandulifera*: from foe to friend? Sustainability. 11(18):5018-5035. doi:10.3390/su11185018.
- COLLA G, ROUPHAEL Y. 2009. Evaluation of saffron (*Crocus sativus* L.) production in Italy: effects of the age of saffron fields and plant density. J Food Agric Environ. 7(1):19-23. https://www.researchgate.net/publication/268268074_Evaluation_of_saffron_Crocus_sativus_L_production_in_Italy_Effects_of_the_age_of_saffron_fields_and_plant_density.
- DONG M, XUE X, YANG H, LI Z. 2017. Highly cost-effective shielding composite made from vanadium slag and boron-rich slag and its properties. Rad Phys Chem. 141:239-244. doi:10.1016/j.radphyschem.2017.07.023.
- DYBCZYŃSKI RS. 2019. The role of NAA in securing the accuracy of analytical results in the inorganic trace analysis. J Radioanal Nucl Ch. 322:1505-1515. doi:10.1007/s10967-019-06675-7.
- ESNA-ASHARI M, GHOLAMI M. 2010. The effect of increased chloride (Cl-) content in nutrient solution on yield and quality of strawberry (*Fragaria ananassa* Duch.) fruits. J Fruit Ornament Plant Res. 18(1):37-44. http://www.insad.pl/jofaop.html.
- [FAO] Food and Agriculture Organization. 2006. Plant nutrition for food security: a guide for integrated nutrient management. Rome, Italy: Food and Agriculture Organization of the United Nations (FAO).
- FRANCO-NAVARRO JD, BRUMÓS J, ROSALES MA, CUBERO-FONT P, TALÓN M, COLMENERO-FLORES JM. 2015. Chloride regulates leaf cell size and water relations in tobacco plants. J Exp Bot. 67 (3):873-891. doi:10.1093/jxb/erv502.
- HOSSEINI A, RAZAVI BM, HOSSEINZADEH H. 2018. Saffron (*Crocus sativus*) petal as a new pharmacological target: a review. Iran J Basic Med Sci. 21(11):1091-1099. doi:10.22038/IJBMS.2018.31243.7529.
- ITA RE, ANWANA ED. 2017. Geochemical assessment of heavy metal contamination in rural and urban wetlands in Akwa Ibom State, Nigeria. New York Sci J. 10(11):43-51. doi:10.7537/marsnys101117.06.
- JOSE J, SRIMURUGANANDAM B. 2020. Investigation of road dust characteristics and its associated health

- risks from an urban environment. Environ Geochem Health. 42:2819-2840. doi:10.1007/s10653-020-00521-6.
- KABATA-PENDIAS A. 2011. Trace elements in soils and plants: fourth editions. Boca Raton (FL): CRC Press, Taylor & Francis Group. doi:10.1201/b10158.
- KAZI TG, BRAHMAN KD, BAIG JA, AFRIDI HI. 2019. Bioaccumulation of arsenic and fluoride in vegetables from growing media: health risk assessment among different age groups. Environ Geochem Health. 41:1223-1234. doi:10.1007/s10653-018-0207-8.
- KŁOS A, RAJFUR M, WACŁAWEK M. 2011. Application of enrichment factor (EF) to the interpretation of results from the biomonitoring studies. Ecol Chem Eng S. 18(2):171-183. https://www.researchgate.net/publication/266039475_Application_of_enrichment_factor_EF_to_the_interpretation_of_results_from_the_biomonitoring_studies.
- KOOCHEKI A, SEYYEDI SM. 2015. Phonological stages and formation of replacement corms of saffron (*Crocus sativus* L.) during growing period. J Saffron Res. 3(2):134-154. doi:10.22077/JSR.2015.290.
- KOWALSKA JB, MAZUREK R, GĄSIOREK M, ZALESKI T. 2018. Pollution indices as useful tools for the comprehensive evaluation of the degree of soil contamination—a review. Environ Geochem He. 40:2395-2420. doi:10.1007/s10653-018-0106-z.
- KUMAR V, KUMAR P, SINGH J, KUMAR P. 2020. Potential of water fern (*Azolla pinnata* R. Br.) in phytoremediation of integrated industrial effluent of SIIDCUL, Haridwar, India: removal of physicochemical and heavy metal pollutants. Int J Phytoremediation. 22(4):392-403. doi:10.1080/15226514.2019.1667950.
- LI R, WU H, DING J, FU W, GAN L, LI Y. 2017. Mercury pollution in vegetables, grains and soils from areas surrounding coal-fired power plants. Sci Rep. 2017:46545. doi:10.1038/srep46545.
- MÁDLÍKOVÁ M, KRAUSOVÁ I, MIZERA J, TÁBORSKÝ J, FAMĚRA O, CHVÁTIL D. 2018. Nitrogen assay in winter wheat by short-time instrumental photon activation analysis and its comparison with the Kjeldahl method. J Radioanal Nucl Chem. 317:479-486. doi:10.1007/s10967-018-5881-6.
- MALEKZADEH SHAFAROUDI A, BOROZINIAT B, HAIDARIAN SHAHRI MR. 2022. Integration of

- geological and geophysical studies in order to mineral exploration at the Zaveh mineralization area, NE Iran. Iran J Earth Sci. 14(2):150-164. doi:10.30495/IJES.2021.685384.
- MALINOWSKA E, JANKOWSKI K, WIŚNIEWSKA-KADŻAJAN B, SOSNOWSKI J, KOLCZAREK R, JANKOWSKA J, CIEPIELA GA. 2015. Content of zinc and copper in selected plants growing along a motorway. Bull Environ Contam Toxicol. 95(5):638-643. doi:10.1007/s00128-015-1648-8.
- MARÍN S, PARDO O, BAGUENA R, FONT G, YUSÀ V. 2017. Dietary exposure to trace elements and health risk assessment in the region of Valencia, Spain: a total diet study. Food Addit Contam Part A Chem Anal Control Expo Risk Assess. 34(2):228-240. doi:10.1080/19440049.2016.1268273.
- MASTO RE, SINGH MK, ROUT T, KUMAR A, KUMAR S, GEORGE J, SELVI VA, DUTTA P, TRIPATHI RC, SRIVASTAVA NK. 2019. Health risks from PAHs and potentially toxic elements in street dust of a coal mining area in India. Environ Geochem He. 41:1923-1937. doi:10.1007/s10653-019-00250-5.
- MCKENNA E, THOMPSON KA, TAYLOR-EDMONDS L, MCCURRY DL, HANIGAN D. 2020. Summation of disinfection by-product CHO cell relative toxicity indices: sampling bias, uncertainty, and a path forward. Environ Sci: Processes Impacts. 22:708-718. doi:10.1039/C9EM00468H.
- [MHPRC] Ministry of Health of the People's Republic of China. 2012. Maximum levels of contaminants in foods GB2762-2012. Beijing, China: China State Environmental Protection Administration.
- MINC L. 2008. Neutron activation analysis. In: Pearsall DM, editor. Encyclopedia of archaeology. Academic Press. p. 1669-1683.
- MISDAQ MA, BOURZIK W. 2004. Evaluation of annual committed effective doses to members of the public in Morocco due to 238U and 232Th in various food materials. J Radiol Prot. 24(4):391-399. doi:10.1088/0952-4746/24/4/003.
- MOHD-TAUFEK N, CARTWRIGHT D, DAVIES M, HEWAVITHARANA A, KOORTS P, MCCONACHY H, SHAW P, SUMNER R, WHITFIELD K. 2016. The effect of pasteurization on trace elements in donor breast milk. J Perinatol. 36(10):897-900. doi:10.1038/jp.2016.88.

- MONDAL P, SCHINTU M, MARRAS B, BETTOSCHI A, MARRUCCI A, SARKAR SK, CHOWDHURY R, JONATHAN MP, BISWAS JK. 2020. Geochemical fractionation and risk assessment of trace elements in sediments from tide-dominated hooghly (Ganges) River Estuary, India. Chem Geol. 532:119373.
- MORATALLA-LÓPEZ N, BAGUR MJ, LORENZO C, SALINAS M, ALONSO GL. 2019. Bioactivity and bioavailability of the major metabolites of *Crocus sativus* L. flower. Molecules. 24(15):2827. doi:10.3390/molecules24152827.
- NEPOMUCENO RA, BROWN CB, GARGARINO AMP, PEDRO MS, BROWN MB. 2020. Growth enhancement of rice (*Oryza sativa* L.) by zincsolubilizing bacteria isolated from Vesicular-Arbuscular Mycorrhizal Root Inoculant (VAMRI). Philipp J Crop Sci. 45(1):34-40. https://ovcre.uplb.edu.ph/journals-uplb/index.php/PJCS/article/view/372/347.
- NOURALIEE J. 2005. Preliminary exploration of geothermal resources in Khorasan Province, NE-Iran. Proceedings of the World Geothermal Congress; 24-29 Apr 2005; Antalya, Turkey. p. 1-8. https://www.geothermal-energy.org/pdf/IGAstandard/WGC/2005/2607.pdf.
- OMONIYI IM, OLUDARE SMB, OLUWASEYI OM. 2013. Determination of radionuclides and elemental composition of clay soils by gamma-and X-ray spectrometry. SpringerPlus. 2:74. doi:10.1186/2193-1801-2-74.
- OUFNI L, TAJ S, MANAUT B, EDDOUKS M. 2011. Transfer of uranium and thorium from soil to different parts of medicinal plants using SSNTD. J Radioanal Nucl Chem. 287:403-410. doi:10.1007/ s10967-010-0888-7.
- PARR RM. 1984. On the need for improved quality assurance in biomedical neutron activation analysis as revealed by the results of some recent IAEA intercomparisons. In: Quality assurance in biomedical neutron activation analysis. Vienna: International Atomic Energy Agency (IAEA). Report No.: IAEA-TECDOC-323. https://inis.iaea.org/collection/NCLCollectionStore/_Public/16/026/16026143.pdf? r=1&r=1. p. 53-71.

- PIRRONE N, CINNIRELLA S, FENG X, FINKELMAN RB, FRIEDLI HR, LEANER J, MASON R, MUKHERJEE AB, STRACHER G, STREETS DG, ET AL. 2010. Global mercury emissions to the atmosphere from natural and anthropogenic sources. Atmos Chem Phys. 10:5951-5964. doi:10.5194/acp-10-5951-2010.
- RAI PK, LEE SS, ZHANG M, TSANG YF, KIM KH. 2019. Heavy metals in food crops: health risks, fate, mechanisms, and management. Environ Int. 125:365-385. doi:10.1016/j.envint.2019.01.067.
- RASHEED H, SLACK R, KAY P. 2016. Human health risk assessment for arsenic: a critical review. Crit Rev Environ Sci Tech. 46(19-20):1529-1583. doi:10.1080/10643389.2016.1245551.
- REMEIKAITĖ-NIKIENĖ N, GARNAGA-BUDRĖ G, LUJANIENĖ G, JOKŠAS K, STANKEVIČIUS A, MALEJEVAS V, BARISEVIČIŪTĖ R. 2018. Distribution of metals and extent of contamination in sediments from the south-eastern Baltic Sea (Lithuanian zone). Oceanologia. 60(2):193-206. doi:10.1016/j.oceano.2017.11.001.
- ROUT G, SAMANTARAY S, DAS P. 2001. Aluminium toxicity in plants: a review. Agronomie. 21(1):3-21. doi:10.1051/agro:2001105.
- SALOMONS W, FÖRSTNER U. 1984. Metals in continental waters. In: Metals in the hydrocycle. Brühlsche Universitätsdruckerei, Germany: Springer. p. 138-212.
- SAYFI P, NIKBAKHT M. 2016. Identification and ranking green supplier selection criteria using one-sample *T*-test and FANP methods: a case study for petrochemical industry. J Mod Proc Manuf Prof. 5:53-67.
- SHIMIZU K, SAAL AE, MYERS CE, NAGLE AN, HAURI EH, FORSYTH DW, KAMENETSKY VS, NIU Y. 2016. Two-component mantle melting-mixing model for the generation of mid-ocean ridge basalts: implications for the volatile content of the Pacific upper mantle. Geochim Cosmochim Ac. 176:44-80. doi:10.1016/j.gca.2015.10.033.
- SHTANGEEVA I, NIEMELÄ M, PERÄMÄKI P, RYUMIN A, TIMOFEEV S, CHUKOV S, KASATKINA G. 2017. Phytoextration of bromine from contaminated soil. J Geochem Explor. 174:21-28. doi:10.1016/j.gexplo.2016.03.012.

- SINGH S, TRIPATHI DK, SINGH S, SHARMA S, DUBEY NK, VACULÍK M. 2017. Toxicity of aluminium on various levels of plant cells and organism: a review. Environ Exp Bot. 137:177-193. doi:10.1016/j.envexpbot.2017.01.005.
- SLOTKIN TA, SKAVICUS S, STAPLETON HM, SEIDLER FJ. 2017. Brominated and organophosphate flame retardants target different neurodevelopmental stages, characterized with embryonic neural stem cells and neuronotypic PC12 cells. Toxicology. 390:32-42. doi:10.1016/j.tox.2017.08.009.
- STAHL T, TASCHAN H, BRUNN H. 2011. Aluminium content of selected foods and food products. Environ Sci Eur 23:37. doi:10.1186/2190-4715-23-37.
- SYAHFITRI WYN, KURNIAWATI S, ADVENTINI N, DAMASTUTI E, LESTIANI DD. 2017. Macro elemental analysis of food samples by nuclear analytical technique. Journal of physics: conference series. International Nuclear Science and Technology Conference; 6 Aug 2016; Bangkok, Thailand: IOP Publishing Ltd. p. 012023.
- TOHIDI Z, BAGHIZADEH A, ENTESHARI S. 2015. The effects of aluminum and phosphorous on *Brassica napus*. American-Eurasian J Agric Environ Sci. 6 (2):137-142. https://www.researchgate.net/publication/233904467_The_effects_of_Aluminum_and_Phosphorous_on_Brassica_napus.
- TOUSI ET. 2020. Evaluation of levels of some trace metals in *Crocus sativus* L. and their transfer trend from soil to saffron by using neutron activation analysis. Saffron Agron Tech. 8(3):377-397. https://www.researchgate.net/publication/352786744_Evaluation_of_levels_of_some_trace_metals_in_Crocus_sativus_L_and_their_transfer_trend_from_soil_to_saffron_by_using_neutron_activation_analysis.
- TOUSI ET. 2022a. Determining the mobility of some essential elements in saffron (*Crocus sativus* L.) by the neutron activation analysis. Baghdad Sci J. 19:283. doi:10.21123/bsj.2022.19.2.0283.
- TOUSI ET. 2022b. Monte Carlo simulation of the mass attenuation coefficient and effective atomic number of the *Eremurus-Rhizophora* ssp. particleboard phantom at the mammography energy range. Prog Nucl Energ. 149:104281. doi:10.1016/j.pnucene.2022.104281.

- TOUSI ET, ABOARRAH A, BAUK S, HASHIM R, JAAFAR MS. 2018. Measurement of percentage depth dose and half value layer of the *Rhizophora* spp. particleboard bonded by *Eremurus* spp. to 60, 80 and 100 kVp diagnostic x-rays. MAPAN. 33:321-328. doi:10.1007/s12647-018-0257-5.
- TOUSI ET, BAUK S, HASHIM R, JAAFAR MS, ABUARRA A, ALDROOBI KSA, AL-JARRAH AM. 2014. Measurement of mass attenuation coefficients of *Eremurus-Rhizophora* spp. particleboards for x-ray in the 16.63–25.30 keV energy range. Radiat Phys Chem. 103:119-125. doi:10.1016/j.radphyschem.2014.03.011.
- TOUSI ET, FIROOZABADI MM, SHIVA M. 2016. Determination of the thorium potential in Shah-Kooh area in Iran by NAA and comparison with the results of ICP and XRF techniques. Measurement. 90:20-24. doi:10.1016/j.measurement.2016.04.020.
- TOUSI ET, HASHIM R, BAUK S, JAAFAR MS. 2017. Evaluation of the mass attenuation coefficient and effective atomic number of the *Eremurus* spp. root in mammography energy range. IOSR J Appl Phys. 9 (1):100-104. doi:10.9790/4861-090101100104.
- TOUSI ET, HASHIM R, BAUK S, JAAFAR MS, ABUARRA AMH, AL-JARRAH AM, ABABNEH B, TOUSI AT, ALDROOBI KSA. 2015. Characterization of the *Rhizophora* particleboard as a tissue-equivalent phantom material bonded with bio-based adhesive. Maderas-Cienc Tecnol. 17:305-318. doi:10.4067/S0718-221X2015005000029.
- TOUSI ET, HASHIM R, BAUK S, JAAFAR MS, AL-JARRAH AM, KARDANI H, ABUARRA A, HAMDAN AM, ALDROOBI KSA. 2014. A study of the properties of animal-based wood glue. Adv Mat Res. 935:133-137. doi:10.4028/www.scientific.net/ AMR.935.133.
- TOUSI ET, KARDANI H, FIRUZABADI MM, JAAFAR MS, ALJARRAH AM, GHASEMI L, KHANIABADI PM, AMIN YA. 2014. Shielding design for an Am-Be neutron source using MCNP4C code and real dosimetry. Caspian J Appl Sci Res. 3:13-22.
- [USGS] U.S. Geological Survey. 2023. Neutron activation analysis. https://www.usgs.gov/usgs-triga-reactor/neutron-activation-analysis.

- WHITE PJ, BROADLEY MR. 2001. Chloride in soils and its uptake and movement within the plant: a review. Ann Bot-London. 88(6):967-988. doi:10.1006/anbo.2001.1540.
- [WHO] World Health Organization. 2000. Evaluation of certain food additives and contaminants. Technical report series: 896. Geneva, Switzerland: World Health Organization.
- [WHO] World Health Organization. 2003. Chlorine in drinking water: background document for development of WHO guidelines for drinking water quality. Geneva, Switzerland: World Health Organization.
- [WHO] World Health Organization. 2011. Guidelines for drinking-water quality, 4th edition. Geneva, Switzerland: World Health Organization.
- [WHO] World Health Organization, Joint FAO/WHO Expert Committee on Food Additives, [FAO] Food and Agriculture Organization of the United Nations. 2018. Evaluation of certain veterinary drug residues in food: eighty-fifth report of the Joint FAO/WHO Expert Committee on Food Additives. World Health Organization. https://apps.who.int/iris/handle/10665/259895. License: CC BY-NC-SA 3.0 IGO.
- WYCZARSKA-KOKOT J, LEMPART A, DUDZIAK M. 2017. Chlorine contamination in different points of pool-risk analysis for bathers' health. Ecol Chem Eng-A. 24(2):217-226. doi:10.2428/ecea.2017.24(2)23.

- YAFFEE AQ, SCOTT B, KAELIN C, CAMBRON J, SANDERSON W, CHRISTIAN WJ, MORAN TP, CHAMNESS J. 2019. Collaborative response to arsenic-contaminated soil in an Appalachian Kentucky neighborhood. J Toxicol Env Heal A. 82 (12):697-701. doi:10.1080/15287394.2019.1641872
- ZAICHICK V, ZAICHICK S. 2016. Trace element contents in adenocarcinoma of the human prostate gland investigated by neutron activation analysis. Cancer Res Oncol. Cancer Research and Oncology, 1, 1-10.
- ZEHRINGER M. 2020. Monitoring of natural radioactivity in drinking water and food with emphasis on alpha-emitting radionuclides. In: Osibote OA, editor. Ionizing and non-ionizing radiation. London, UK: InTech Open. p. 551-561.
- ZHAO K, XUE H, ZHAO LY. 2019. Research on the micro-mechanical state at tip of environmentally assisted cracking based on Latin hypercube sampling method. Key Eng Mat. 795:74-78. doi:10.4028/www.scientific.net/KEM.795.74.
- ZINKUTĖ R, TARAŠKEVIČIUS R, JANKAUSKAITĖ M, STANKEVIČIUS Ž. 2017. Methodological alternatives for calculation of enrichment factors used for assessment of topsoil contamination. J Soil Sediment. 17:440-452. doi:10.1007/s11368-016-1549-4.